Lithos 344–345 (2019) 86–99

Contents lists available at ScienceDirect

Lithos

journal homepage: www.elsevier.com/locate/lithos

Zirconium in rutile thermometry of the Himalayan ultrahigh-pressure eclogites and their retrogressed counterparts, Kaghan Valley, Pakistan

Hafiz Ur Rehman [a,*], Yoshiyuki Iizuka [b], Hao-Yang Lee [b], Sun-Lin Chung [b,c], Zhanzhan Duan [d], Chunjing Wei [d], Tahseenullah Khan [e], Tehseen Zafar [f], Hiroshi Yamamoto [a]

[a] Graduate School of Science and Engineering, Kagoshima University, Kagoshima 890-0065, Japan
[b] Institute of Earth Sciences, Academia Sinica, Taipei, Taiwan
[c] Department of Geosciences, National Taiwan University, Taipei, Taiwan
[d] MOE Key Laboratory of Orogenic Belts and Crustal Evolution, School of Earth and Space Sciences, Peking University, Beijing 100871, China
[e] Department of Earth and Environmental Sciences, Bahria University, Islamabad, Pakistan
[f] State Key Laboratory of Ore Deposit Geochemistry, Institute of Geochemistry, Chinese Academy of Sciences, Guiyang 550081, China

ARTICLE INFO

Article history:
Received 27 December 2018
Received in revised form 10 June 2019
Accepted 14 June 2019
Available online 19 June 2019

Keywords:
Zr-in-rutile thermometry
Himalaya
Kaghan Valley
UHP eclogites
Garnet-amphibolites

ABSTRACT

This study reports zirconium-in-rutile thermometry data from the Himalayan ultrahigh-pressure eclogites and their retrogressed counterparts. The Zr contents of three textural varieties of rutile i.e. matrix rutile, inclusion phase, and overgrown by ilmenite/titanite from coesite-bearing eclogites, slightly retrogressed eclogites, highly retrogressed eclogites, and amphibolites were analyzed for Zr contents using the electron probe micro-analyser. Majority of the rutile grains exhibited homogeneous chemical compositions in all the aforementioned textural varieties; however, some of grains were relatively heterogeneous. Average temperature values of 729 °C, 727 °C, and 706 °C were obtained for the matrix, inclusion, and overgrown rutiles from UHP eclogites and of 705 °C, 699 °C, and 707 °C for those from HP eclogites, respectively. Slightly retrogressed eclogites yielded similar average T values of 703 °C, 706 °C, and 706 °C, respectively, whereas highly retrogressed eclogites resulted in relatively low average temperatures, ca. 690 °C, 691 °C, and 679 °C, respectively. When compared with these eclogites, lower average T values of 672 °C, 630 °C, and 656 °C were obtained from garnetites, and of 665 °C, 658 °C, and 640 °C from garnet amphibolites, respectively. The relatively homogeneous Zr contents and higher temperature values from the matrix rutile in HP and UHP eclogites suggest peak or near-peak metamorphic crystallization, whereas grains with low Zr contents, yielding low temperature values, were likely to be affected by the late-stage retrogression.

1. Introduction

Subduction-related high−/ultrahigh-pressure (HP/UHP) metamorphic rocks are composed of silicate minerals e.g., garnet, pyroxene, white mica, and amphibole that provide information regarding the pressure–temperature–time (P–T–t) conditions under which they from, recrystallize, or chemically exchange major and trace elements among them during metamorphic evolution. In major elements, the Fe-Mg exchange thermometer is commonly used between the coexisting phases, such as garnet and clinopyroxene or garnet and phengite, to constrain the P–T conditions (Green and Helman, 1982; Krogh Ravna, 1988; Krogh Ravna and Raheim, 1978; Krogh Ravna and Terry, 2004; Powell and Holland, 2008). Several thermometers, barometers (for details see Spear, 1993), and computer programs such as THERMOCALC (Holland and Powell, 1998, 2006; Powell et al., 1998; Powell and Holland, 2008), PERPLEX (Connolly, 1990, 2005, 2009), and THERIAK-DOMINO (de Capitani and Brown, 1987; de Capitani and Petrakakis, 2010) are used to estimate the prograde, peak and retrograde metamorphic conditions in rocks (Wei et al., 2003; Wei and Tian, 2014). To determine the P–T estimations, the texturally coexisting phases (considered to be in equilibrium) are analyzed for their major elements without determining the valence state of those elements. The estimation of metamorphic temperatures, particularly in case of the HP and UHP rocks, may be subject to systematic errors if the entire Fe content is considered to be ferrous (e.g., Hacker, 2006; Stípská and Powell, 2005). Fortunately, some accessory phases, such as rutile or zircon can be used for independent temperature estimations. Rutile incorporates significant amount of high field strength elements (such as Zr, Hf, Nb, and Ta) during its growth/recrystallization in subduction-related environments. The incorporation of Zr into rutile is temperature-dependent in the zircon- and quartz-buffered assemblages as reflected by the systematic differences observed in Zr concentration in rutile from medium-temperature eclogites to

* Corresponding author.
E-mail address: hafiz@sci.kagoshima-u.ac.jp (H.U. Rehman).

https://doi.org/10.1016/j.lithos.2019.06.017
0024-4937/

high-temperature granulites (Luvizotto et al., 2009; Luvizotto and Zack, 2009; Miller et al., 2007; Tomkins et al., 2007; Watson et al., 2006; Zack et al., 2002; Zack et al., 2004; Zack and Kooijman, 2017). Experimental studies confirmed the pressure-dependency of Zr-in-rutile, therefore, it is suitable for obtaining precise temperature estimates for rutile crystallization in natural rocks (Degeling et al., 2002; Ewing et al., 2013; Ferry and Watson, 2007; Pape et al., 2016; Tomkins et al., 2007; Watson et al., 2006). Zack et al. (2004) observed that the Zr-in-rutile thermometry results were consistent with the conventional thermobarometry results for crustal lithologies metamorphosed from 430 to 1100 °C. Zack and Luvizotto (2006) extended this work to eclogites exhibiting a temperature range of 400–900 °C and the results were within 25 °C difference from conventional thermobarometry. Tomkins et al. (2007) experimental work on the ZrO_2 solubility in rutile coexisting with zircon and quartz, for P = 1 atm, 10, 20, and 30 kbar, and T between 1000 and 1500 °C, found that the Zr contents in rutile increased as the T increased and P decreased, suggesting pressure-dependence on Zr-in-rutile thermometry. Many subsequent studies yielded promising results, suggesting that the single mineral thermometer is a useful tool for metamorphic temperature estimates and petrochronology (e.g., Cruz-Uribe et al., 2018; Ewing et al., 2013; Jiao et al., 2011; Kohn et al., 2016; Kooijman et al., 2012; Pape et al., 2016; Taylor et al., 2016; Tual et al., 2018; Zack and Kooijman, 2017 and references therein).

A few case studies on mafic rocks produced Zr-in-rutile temperatures consistent with the previously published temperature data obtained from conventional thermobarometry. Examples include the Ivrea-Verbano Zone (IVZ) granulites (Ewing et al., 2013; Pape et al., 2016), the UHT Napier Complex granulites, Antarctica (Harley, 2008), the Chinese Continental Scientific Drilling (CCSD) main hole eclogites (Zhang et al., 2009), the granulites of the Khondalite Belt (KB), China (Jiao et al., 2011), the granulites of the Canadian Archean Pikwitonei Granulite (APG) Domain (Kooijman et al., 2012), the garnet-clinopyroxene granulite of the Bohemian Massif (BM) (Usuki et al., 2017), and the Sweconorwegian orogen eclogites (Tual et al., 2018). Jiao et al. (2011) observed bimodal Zr-in-rutile concentrations in the granulites of the KB, where the high T values in Zr-rich rutile were interpreted for peak granulite facies metamorphism, and the low T values in Zr-poor rutile were attributed to late-stage cooling. Pape et al. (2016) reported that most of the rutile preserved peak metamorphic temperatures and some of the grains were affected by the post-peak metamorphic modification because of Zr-diffusion. Majority of the aforementioned studies indicate that Zr-in-rutile thermometry produces robust results, however, questions remain regarding the extent to which the rutile grains in most of the metamorphic rocks retain primary (peak metamorphic) Zr concentrations or have been modified by the subsequent thermal events.

The above studies indicate that the Zr concentrations within individual grains tend to be homogeneous and that chemical variations between grains are not uncommon even though these variations are not always obviously associated with the texture, which pose difficulties for interpreting the results. This suggests that rutile may grow under different P–T conditions, form at different times, experience different diffusional rates along the grain-boundaries, or be affected by the fluid-controlled diffusions at the individual grain level. The process occurred in specific cases is unclear, however, the common consensus is that the maximum Zr contents in rutile represent minimum peak metamorphic temperatures, whereas lower Zr contents reflect late-stage cooling (e.g., Ewing et al., 2013; Kooijman et al., 2012; Miller et al., 2007; Pape et al., 2016; Zack and Kooijman, 2017; Zack and Luvizotto, 2006).

We present a case study from the Himalayan metamorphic belt, Kaghan Valley, Pakistan. Texturally different types of rutile grains were investigated from rock samples that exhibit a broad P–T range with a multi-stage metamorphic history; some preserved the UHP eclogites facies conditions, whereas others underwent different degrees of retrogression, and one sample of garnet-amphibolites showed no evidence of the eclogite facies metamorphism. The aim was to extract the peak metamorphic records and to assess the influence of late-stage retrogression on the Zr-in-rutile thermometry.

2. Geological background

The Himalayan metamorphic belt is comprised of metasedimentary rocks intercalated with metabasites of the Indian Plate that experienced a multi-stage evolutionary history via collision/subduction and exhumation processes (Kaneko et al., 2003; Kohn, 2014; O'Brien et al., 2001; Rehman, 2019; Rehman et al., 2007, 2011; Tahirkheli, 1979; Treloar et al., 2003; Wilke et al., 2010 and references therein). The dominant lithotectonic units exposed in the study area from north to south are: (1) the Higher Himalayan Crystalline (HHC), (2) the Lesser Himalayan Sequence (LHS), and (3) the Siwalik group (Molasse) sediments of the Sub-Himalayas (Fig. 1). The HHC comprises Late Proterozoic to Late Paleozoic granitic gneisses basement overlain by psammitic, pelitic and calcareous metasedimentary cover sequences, and is intruded by the dikes and sills of the Permian Panjal Trap flood basalts (Chaudhry and Ghazanfar, 1987; Greco et al., 1989; Greco and Spencer, 1993). Majority of the mafic lithologies are metamorphosed under the eclogite facies conditions in the northeast, near the collision boundary known as the Indus-Tsangpo Suture, whereas those in the southwest (away from the suture) were metamorphosed under the amphibolite facies conditions (Lombardo and Rolfo, 2000; Pognante and Spencer, 1991; Rehman et al., 2017). A steeply dipping regional thrust known as the Batal Thrust or the Main Central Thrust (MCT) separates the HHC from the LHS (Fig. 1). The LHS mainly comprises Proterozoic to Cambrian metasedimentary rocks (calcareous schists, marbles, graphitic and pelitic schists, and quartzite) locally intruded by the Permian Panjal Traps. Majority of these lithologies are metamorphosed under greenschist to amphibolite facies conditions (Chaudhry and Ghazanfar, 1987; Treloar, 1995, 1997). To the south of the Main Boundary Thrust (MBT), unmetamorphosed Miocene to Pleistocene Siwalik group sediments, derived from the erosion of the Himalayan uphill, resulted in the formation of the Sub-Himalayas (Rehman et al., 2017 and references therein).

Our study focused on the rutile grains in the HHC mafic rocks, which preserve the highest metamorphic grades (UHP eclogites) to the north, close to the subduction-collision boundary (Fig. 2). The host felsic gneisses surrounding the UHP metabasite body underwent UHP metamorphism, indicated by the coesite inclusions in zircon (Kaneko et al., 2003). These features suggest that the mafic bodies are not exotic blocks but are part of a large intact unit, forming the leading-edge of the subducting Indian Plate that experienced UHP metamorphism. Mafic rocks that were exposed in the south of the UHP locality experienced weak to strong retrogression, which was evident by the common presence of the albite-quartz symplectites around omphacite in slightly retrogressed eclogites that transform into highly retrogressed eclogites further southwest (Rehman et al., 2007, 2013a, 2017). Garnetites are exposed near the UHP body, but due to the absence of any UHP phase, it is unclear whether the rocks also experienced UHP metamorphism. Further southwest, the amphibolite facies rocks show no evidence of the eclogite facies metamorphism (Rehman et al., 2017).

3. Analytical procedure

Thirteen samples from UHP eclogites, retrogressed eclogites, and amphibolites were selected for this study. Rutile grains within polished thin sections from two UHP eclogites samples (*Ph423 and Ph425*), four HP eclogites (*Ph379, Ph380A, Ph380D, and Ph553*), two samples each from slightly retrogressed eclogites (*Ph312 and Ph326*), highly retrogressed eclogites (*Ph241 and Ph243*), and garnetites (*Ph4534 and Ph537*), and one garnet-amphibolite sample (*Ph482*) were investigated for textural features. Three textural varieties of rutile were identified:

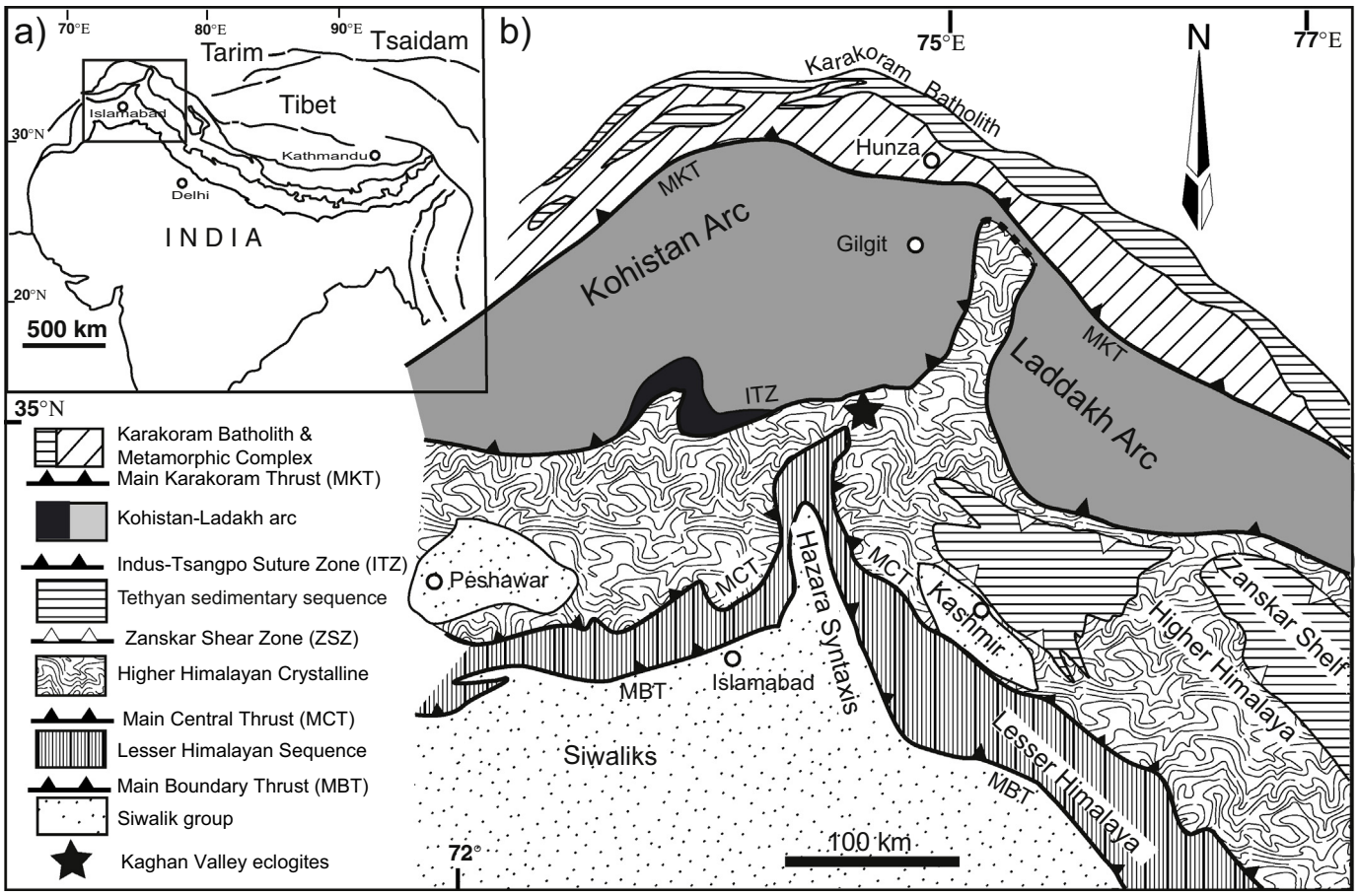

Fig. 1. (a) A simplified sketch of the Himalayan mountain range (the rectangular box represents the western part of the Himalayas). (b) A simplified geological map of the western Himalayas that displays the northern part of the Asian Plate, the Kohistan–Ladakh island arc, and lithologies of the Indian Plate (modified after Gansser, 1964; Tahirkheli, 1979; Searle et al., 1999; Kaneko et al., 2003; Rehman et al., 2007). The filled star denotes the location of the Kaghan Valley.

individual grains in the matrix termed as Rt_{mtx}, inclusions in garnet (and a few in omphacites in eclogites) termed as Rt_{inc}, and overgrown by ilmenite or titanite termed as Rt_{ovg}. No evidence of multiple domains in rutile was observed in the investigated samples.

In-situ analysis on the three textural types of rutile were conducted for five elements (Si, Ti, O, Nb and Zr) using the field emission electron probe micro-analyser (JEOL JXA-8500F) at the Institute of Earth Sciences (IES), Academia Sinica, Taipei, with an acceleration voltage of 18 kV, beam current of 100 nA, and beam diameter of 2 um. Counting time for analysis was 10 s (with 5 s background) for Si, Ti and O, and 200 s (with 30 s background) for Nb and Zr, respectively. For quality control and to assess the elemental contamination from surrounding silicate phases or submicron zircon inclusions within rutile, Si and Zr contents were monitored and data that had anomalously high Si or Zr contents were discarded. The quantitative data were corrected using the metal PR-ZAF method (Reed, 1993). Standards used were kyanite for Si, synthetic rutile (Zr- and Nb-free) for Ti and O, Nb-metal for Nb, and Ti- and Nb-free zircon for Zr. Calibrations for Zr measurements were confirmed by the rutile standards (Diss: 97.8 ppm, R19: 264.4 ppm, and R10: 768.9 ppm) of Luvizotto et al. (2009) and the results were within ±10% error. Detection limits, based on the standard calibration, were ~30 ppm for Zr and Nb, and ~10 ppm for Si, and Ti.

4. Description and petrography of the samples

Detailed petrography, mineral paragenesis, and results of conventional thermobarometry (excluding garnet-amphibolites and garnetites) were reported in Rehman et al. (2007, 2008, 2013b), geochemistry and protolith-related information in Rehman et al. (2008, 2013a), and U-Pb zircon age, Hf and oxygen isotope data in Rehman et al. (2014, 2016, 2018). For the ease of readers, we review simplified textural features for the studied samples herein. Locations of the rock samples are given in Fig. 2 and the petrographic details are provided in Table 1.

(1) Ultrahigh-pressure (UHP) eclogites occur as boudins or lenses, a few cm to as much as 2 m in diameter, within the UHP felsic gneisses. Garnet aggregates (individual grains measuring 0.2–0.4 mm) coexist with omphacite (0.3–2 mm), and are rimmed by thin (~0.2 mm) hornblende and micron-scale symplectites (Fig. 3a and b). Most of the garnet grains exhibiting no significant chemical zoning and coesite pseudomorphs within omphacite confirm these phases equilibration under UHP conditions. Phengite, epidote, and quartz also occur randomly throughout. Rutile occurs as 50–200 μm grains in the matrix, as <50 μm inclusions in garnet and omphacite, and as 50–350 μm grains overgrown by ilmenite and titanite. Rehman et al. (2007) estimated P–T conditions of 2.8 ± 0.04 GPa and 762 ± 46 °C for the UHP eclogites.

(2) HP eclogites occur as massive sheets or layers ranging from a few meters to several tens of meters thick and extending for a few hundred meters in the east–west direction (for field features refer to Rehman et al., 2017). Felsic gneisses and marbles surround the mafic sheets. These eclogites are medium to coarse grained and comprise garnet, omphacite, quartz, and symplectitic amphibole with rare epidote and accessory zircon, rutile, titanite, and ilmenite (Fig. 3c and d). Garnet grains (0.5–1 mm) display weak chemical (prograde) zoning with

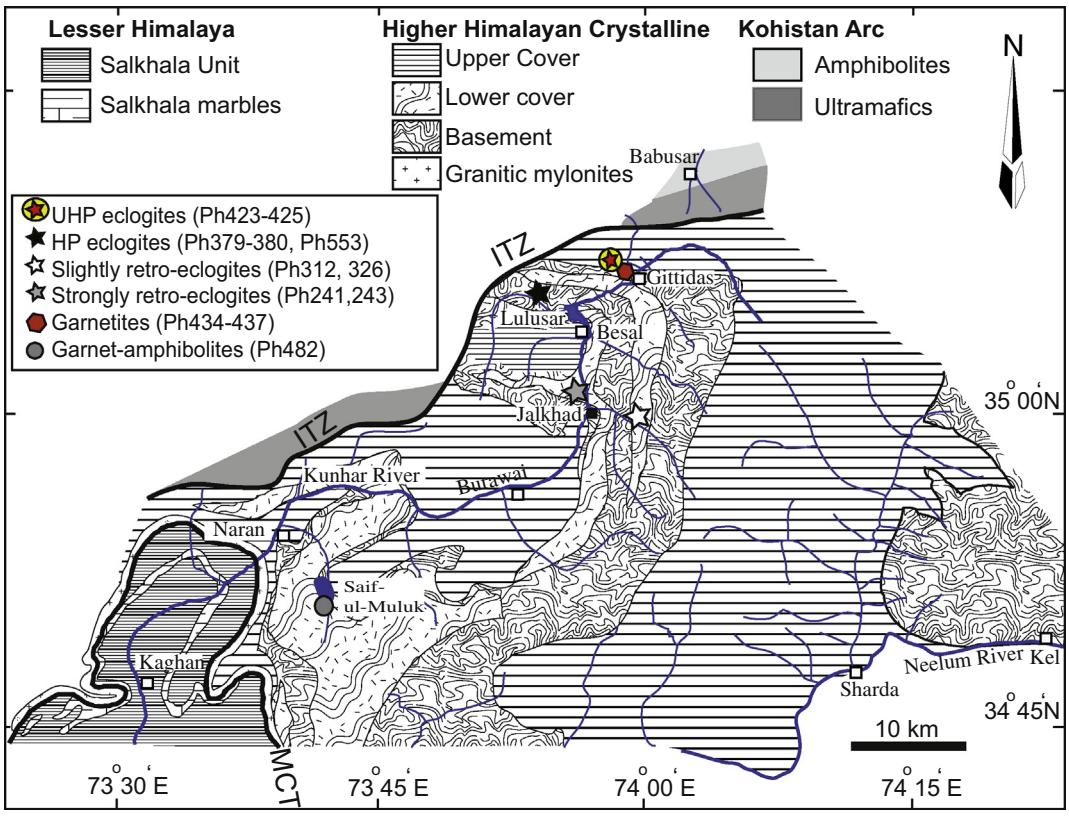

Fig. 2. A geological map of the Kaghan Valley, displaying the locations of the UHP eclogites, retrogressed eclogites, garnetites, and garnet-amphibolites (map modified after Chaudhry and Ghazanfar, 1987; Greco et al., 1989; O'Brien et al., 2001; Kaneko et al., 2003; Rehman et al., 2007, 2017).

Table 1
Sample description, number of analysis in three textural varieties of rutile, and the Zr-in-rutile thermometry results.

Sample	Mineral assemblage	Number of spots analyzed				Average temperatures (°C)			Previous P-T records
		Rt_{mtx}	Rt_{inc}	Rt_{ovg}	Sum	Rt_{mtx}	Rt_{inc}	Rt_{ovg}	(Fe-Mg exchange)
UHP eclogites									
PH423	Grt + Omp + Ph + Ep + Hbl + Qtz/Coe + Rt + Ttn + ilm + Zrn	9	16	2	27	724	725	706	2.8 ± 0.04 GPa, 762 ± 46 °C from UHP eclogite (Ph423 from Rehman et al., 2007)
Ph425	*ditto*	12	8	–	20	733	728	–	
Average						729	727	706	
HP eclogites									
Ph379	Grt + Omp + Ep + Hbl + Qtz + Rt + Ttn + ilm + Zrn	15	2	32	49	706	687	700	2.3 ± 0.4 GPa, 766 ± 107 °C from HP eclogite (Ph491 from Rehman et al., 2013b)
Ph380A	*ditto*	37	–	81	118	709	–	708	
Ph380D	*ditto*	11	–	106	117	693	–	709	
Ph553	*ditto*	27	10	13	50	712	711	711	
Average						705	699	707	
Slightly retrogressed eclogites									
Ph312	Grt + Omp + Hbl + Qtz + Rt + ilm + Zrn	–	26	14	40	–	714	706	1.9 ± 0.3 GPa, 784 ± 61 °C from retrogressed eclogite (Ph312 from Rehman et al., 2007)
Ph326	*ditto*	2	3	–	5	703	697	–	
						703	706	706	
Highly retrogressed eclogites									
Ph241	Grt + Hbl + Ep + Bt + Qtz + Pl + Rt + ilm	30	3	13	46	701	682	683	NA
Ph243	*ditto*	39	2	2	43	679	699	675	
Average						690	691	679	
Garnetites									
Ph534	Grt + Qtz + Hbl + Rt + ilm + Zrn	28	18	1	47	659	640	651	NA
Ph537	*ditto*	1	26	6	33	684	619	661	
Average						672	630	656	
Garnet-amphibolites									
Ph482	Grt + Hbl + Pl + Ep + Qtz + Rt + ilm + Zrn	12	15	13	40	665	658	640	NA

Foot note of Table 1: Abbreviations used for minerals, Bt: biotite, Coe: coesite, Ep: epidote, Grt: garnet, Hbl: hornblende, ilm: ilmenite, Omp: omphacite, Ph: phengite, Pl: plagioclase (including the symplectitic albite), Qtz: quartz, Rt: rutile, Ttn: titanite, Zrn: zircon. See text for average temperatures calculations.

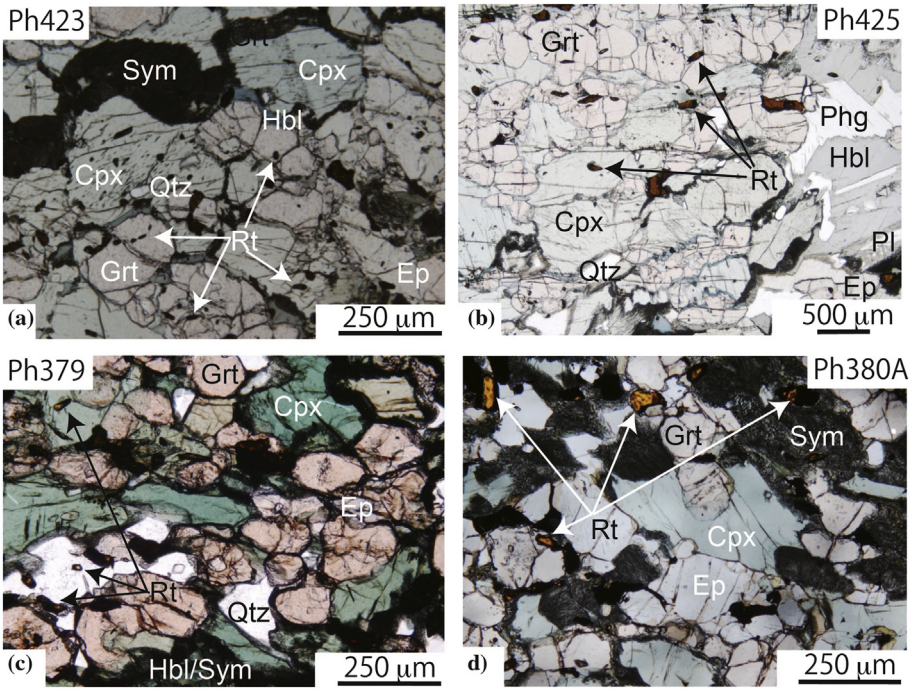

Fig. 3. Photomicrographs (shown in plane polarized light) of the UHP eclogites (a–b) and HP eclogites (c–d). Rutile occurs in the matrix and as inclusions in garnet and omphacite. Rutile overgrown by ilmenite/titanite is also obvious in "d".

quartz, albite, and jadeite inclusions in the relatively Ca-poor and Mn-rich cores and few rutile inclusions in the outer domains (Rehman et al., 2008). Omphacite occurs as 0.2 to 1.5 mm long grains, sharing grain boundaries with garnet and showing retrogression to symplectitic amphibole at certain places (Fig. 3c and d). Further, we observed all the three textural varieties of rutile, among which the most common is the overgrown type (Fig. 3d). Rehman et al. (2013b) estimated the P–T conditions of 2.3 ± 0.4 GPa and 766 ± 107 °C for the HP eclogites.

(3) Slightly retrogressed eclogites occur as layers or sheets with thicknesses of few meters to several tens of meters and are surrounded by felsic/pelitic gneisses and marbles. Modal analysis denoted that these eclogites are >60% garnet grains with less common epidote and hornblende along the grain boundaries

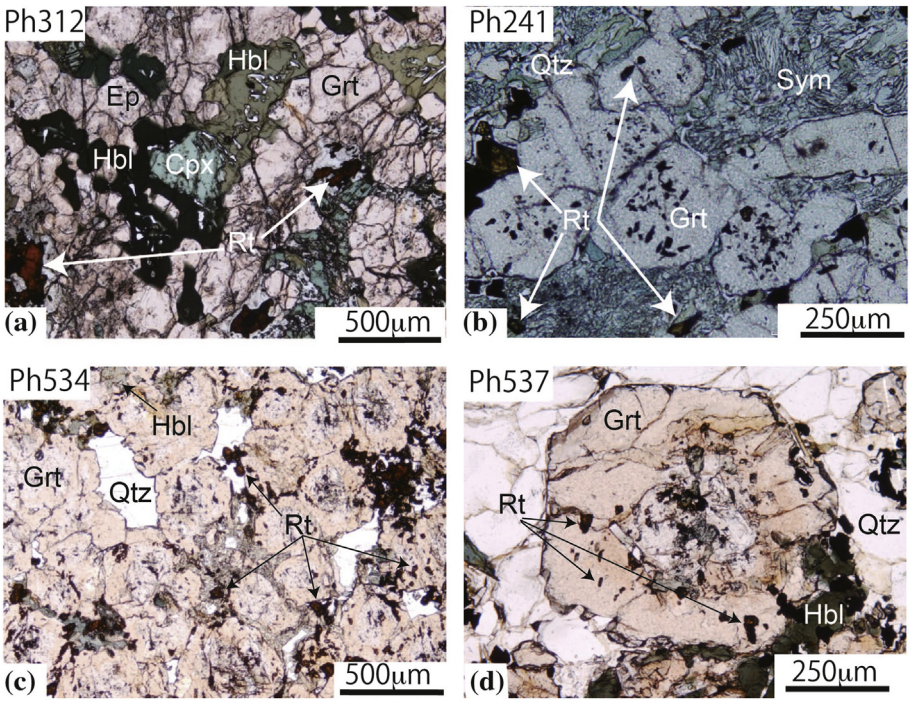

Fig. 4. Photomicrographs displaying the textural features of slightly retrogressed eclogites (a), highly retrogressed eclogites (b), and garnetites (c–d).

and rare local omphacite commonly armored by hornblende (Fig. 4a). Rutile mainly occurred as inclusions in garnet although a few grains were observed in the matrix. Rehman et al. (2007) estimated the P–T conditions to be 1.9 ± 0.3 GPa and 784 ± 61 °C, respectively, for the retrogressed eclogites.

(4) Highly retrogressed eclogites appear as lenses with a thickness of a few meters. They are fine grained with small clustered garnets and commonly contain elongated hornblende, epidote, and quartz. Locally, the garnet grains are surrounded by symplectitic amphibole (Fig. 4b). Tiny rutile and ilmenite randomly occur within the garnet and are sometimes oriented along the foliation. All the three textural varieties of rutile were observed.

(5) A few 2- to 3-m diameter garnetite boudins, hosted by felsic gneisses, are exposed northwest of Gittidas (Fig. 2). Modal analysis showed that these garnetites are almost entirely (>80%) garnet aggregates and remaining (<20%) quartz and amphibole. These clustered garnets display rounded or hexagonal shapes; some grains are optically homogeneous, whereas others have inclusion-poor outer domains but inclusion-rich (darker) and partially resorbed inner cores, resulting in the formation of atoll structures (Fig. 4c). Rutile mainly occurs as inclusions in the outer domains of full (not resorbed) and atoll garnets; the matrix and overgrown varieties are also observed (Fig. 4c and d).

(6) Garnet amphibolites, as 2-m thick dikes or lenticular bodies within pelitic schists and metacarbonates, are exposed in the north of Lake Saiful Muluk (Fig. 2). The central portions of the lenses contain sporadic porphyroblastic garnet (0.3–0.6 mm) in matrix comprised of hornblende, plagioclase, epidote, biotite, and quartz (Fig. 5a and b). The three textural varieties of rutile were observed in this rock.

5. Results

On thirteen polished thin sections, 635 spots were analyzed on three textural varieties of rutile. A summary of the samples, investigated rutile types, and the average temperatures are presented in Table 1. Multiple spots were analyzed in single grains, whereas only a single analysis spot or two were possible on smaller grains (inclusion type rutile). Temperatures were calculated after the calibrations of Tomkins et al. (2007) using the *β-quartz field* for most of the samples (and coesite field for the UHP eclogites). Pressure estimates for the calculations were adopted from the previously determined P–T conditions from conventional thermobarometry (e.g., Rehman et al., 2007, 2013b). For comparison, T values were also calculated according to the calibrations of Zack et al. (2004) and Watson et al. (2006). The values from the calibrations of Tomkins et al. (2007) and Zack et al. (2004) were identical (within ±25 °C) for most of the analyzed grains, however, T values calculated after Watson et al. (2006) were 50 to 70 °C lower. Details of the individual analysis, measured elemental concentrations, and calculated T values are provided in supplementary Table S1 (available on-line).

5.1. UHP Eclogites

In UHP eclogites, 47 spots were analyzed based on the three textural varieties of rutile (Fig. 6a). The Zr contents in *sample Ph423* are 226–391 ppm (average: 290 ppm, *n*: 9) in Rt_{mtx}, 170–418 ppm (average: 297 ppm, *n*: 16) in Rt_{inc}; and only two spots are analyzed in Rt_{ovg} with Zr contents of 205 and 265 ppm (supplementary Table S1). In *sample Ph425*, the Zr contents are 164–392 ppm (average: 324 ppm, *n*: 12) in Rt_{mtx} and 208–418 ppm (average: 306 ppm, *n*: 8) in Rt_{inc}; Rt_{ovg} was not analyzed. Zirconium contents in two UHP samples display a narrow range from 164 to 420 ppm (Fig. 7). Our results are in considerable contrast with the Zr contents of 500–1200 ppm for Sweconorwegian eclogites (Tual et al., 2018), 500–10,500 ppm for the IVZ Alpine eclogites/granulites (Ewing et al., 2013; Pape et al., 2016), 1000–9000 ppm for the BM garnet–pyroxenite granulites (Usuki et al., 2017), and 500–8000 ppm for KB granulites (Jiao et al., 2011).

From *sample Ph423*, the average temperature (T_{ave}) values are 724 °C (range: 703–752 °C) for Rt_{mtx}, 725 °C (680–758 °C) for Rt_{inc}, and 696 °C and 717 °C for Rt_{ovg} (two spots). Similarly, from *sample Ph425*, the T_{ave} values are 733 °C (677–752 °C) for Rt_{mtx} and 728 °C (696–758 °C) for Rt_{inc} (Table 1). The T_{ave} values are within the range of conventional thermobarometry data (760 ± 40 °C) (Fig. 8). The temperature values from the individual grains are relatively homogeneous (within ±25 °C of the T_{ave}), with few grains yielding a larger range but still within ± 50 °C of the T_{ave} (Fig. 9).

5.2. HP Eclogites

In HP eclogites, 334 spots were analyzed using three textural varieties of rutile (representative grains shown in Fig. 6b). The Zr contents in *sample Ph379* are 181–395 ppm (average: 278 ppm, *n*: 15) in Rt_{mtx}, 164–284 ppm (average: 224 ppm, *n*: 2) in Rt_{inc}, and 169–412 ppm (average: 259 ppm, *n*: 32) in Rt_{ovg}. Three other HP eclogite samples yielded 80–530 ppm (Fig. 7; supplementary Table S1).

Although the T_{ave} values from HP eclogites exhibited a wide range when compared with those from the UHP eclogites, majority of the data were within the range obtained from conventional thermobarometry (760 ± 100 °C) (Fig. 8). From *sample Ph379*, the T_{ave} values are 706 °C (673–737 °C) for Rt_{mtx}, 687 °C (two spots: 666 °C and 709 °C) for Rt_{inc}, and 700 °C (674–741 °C) for Rt_{ovg}. Similar T_{ave} data were obtained from rutile in three other HP eclogite samples (Fig. 8; Table 1). Although the temperature data of several individual grains ranged as much as ±50 °C, majority of the data clustered around T_{ave}, mostly falling within ±25 °C (Fig. 9). We did not find any significant chemical variation within the grains (Fig. 10).

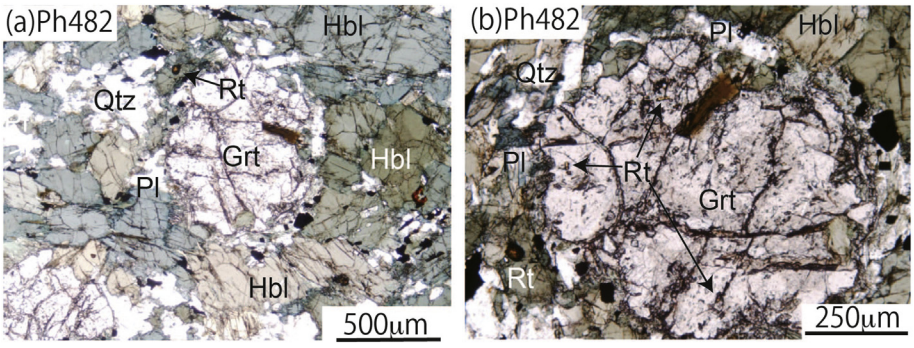

Fig. 5. Photomicrographs displaying the textural features of garnet-amphibolites where the rutile overgrown by ilmenite is visible (a) and zoomed part (b) displaying euhedral garnet grain containing rutile inclusions.

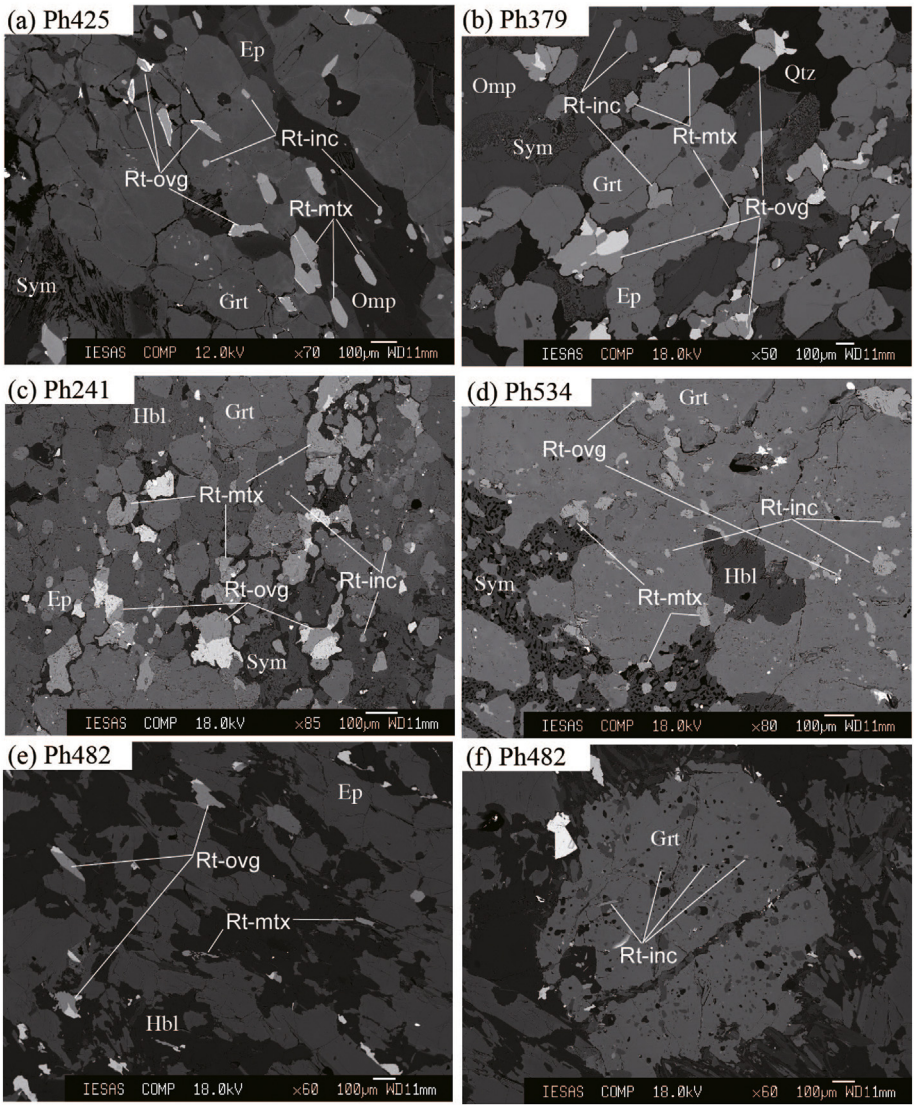

Fig. 6. Backscattered electron images displaying the three textural varieties of rutile in representative samples. (a) UHP eclogites, (b) HP eclogites, (c) highly retrogressed eclogites, (d) garnetites, and (e–f) garnet-amphibolites.

5.3. Slightly retrogressed eclogites

In slightly retrogressed eclogites, 45 spots on three types of rutile were analyzed (Table 1). The Zr contents in Rt_{inc} are 271–474 ppm (average: 363 ppm, *n*: 26), whereas the range in Rt_{ovg} is 168–433 ppm (average: 334 ppm, *n*: 14). The grains from *sample Ph326* yielded 259 and 377 ppm for Rt_{mtx} (*n*: 2) and 276–320 ppm for Rt_{inc} (average: 291 ppm, *n*: 3).

From *sample Ph312*, the T_{ave} values were 714 °C (691–738 °C) for Rt_{inc}, and 706 °C (653–730 °C) for R_{ovg}. Further, similar T values were obtained from rutile in *Sample Ph326* (Fig. 8). The Rt_{inc} temperature values cluster within ±25 °C from the T_{ave}, whereas two Rt_{ovg} grains exhibited a larger range of ±50 °C (Fig. 9).

5.4. Highly retrogressed eclogites

In highly retrogressed eclogites, 89 spots (two samples) on three types of rutiles were analyzed (Table 1). The textural features are depicted in Fig. 6c. The Zr contents in *sample Ph241* are 120–429 ppm (average: 315 ppm, *n*: 30) in Rt_{mtx}, 205–273 ppm (average: 244 ppm, *n*: 3) in Rt_{inc}, and 110–322 ppm (average: 255 ppm, *n*: 13) in Rt_{ovg}. Similar values were obtained from *sample Ph243*.

Sample Ph241 yielded T_{ave} of 701 °C (629–730 °C) for the Rt_{mtx}, 682 °C (669–692 °C) for the Rt_{inc}, and 683 °C (623–705 °C) for the Rt_{ovg}. From *sample Ph243*, T_{ave} is 669 °C (620–728 °C) for the Rt_{mtx}, and two Rt_{inc} grains yielded values of 692 °C and 707 °C, whereas, two other overgrown rutile grains yielded values of 676 °C and 675 °C. These temperature values are lower than those obtained from the HP and UHP eclogites (Fig. 8). The temperature values obtained from individual grains displayed relatively large scatter (Fig. 10), among which the differences were mostly within ±50 °C from T_{ave} but some were as large as ±75 °C (Fig. 9).

5.5. Garnetites

In garnetites, 80 spots (two samples) on three textural varieties of rutiles were analyzed (Table 1). The textural features are depicted in Fig. 6d. In *sample Ph534*, the Zr contents are 86–298 ppm (average: 185 ppm, *n*: 28) in Rt_{mtx} and 45–244 ppm (average: 149 ppm, *n*: 18) in Rt_{inc}; a single Rt_{ovg} grain yielded 162 ppm. In *sample Ph537*, the Zr contents are 33–278 ppm (average: 119 ppm, *n*: 26) in Rt_{inc} and

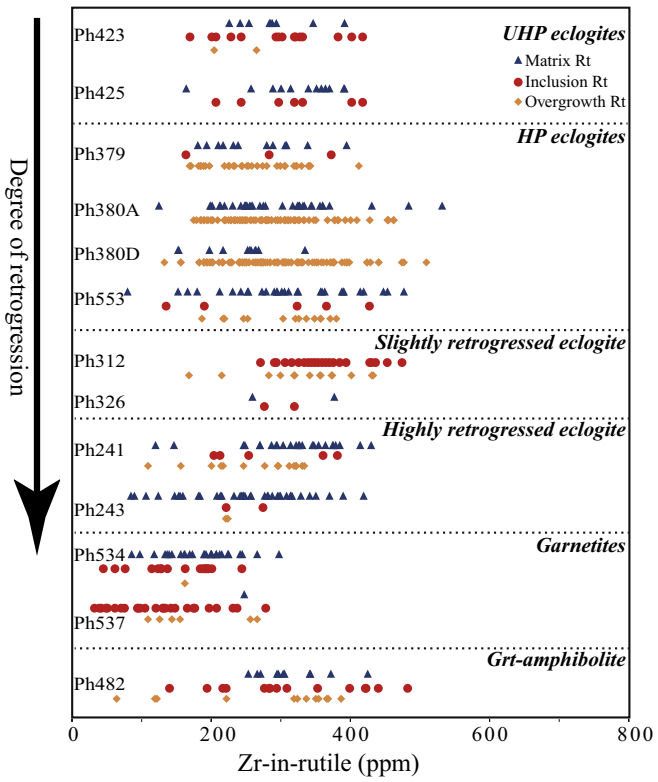

Fig. 7. A diagram displaying the range of Zr contents (ppm) in case of the three textural varieties of rutile from the selected samples. Vertical axis denotes the degree of retrogression (increasing downward). The dashed horizontal lines differentiate different rock suites.

109–266 ppm (average: 186 ppm, *n*: 6) *in* Rt_{ovg}. These Zr contents are lower than those observed in case of rutiles in other samples (Fig. 7); however, the variations within the individual grains are not significant (Fig. 10). The Nb concentration in rutile is notably higher than that in garnetites (3000–8000 ppm) on the basis of a comparison with other samples (supplementary Table S1).

From *sample Ph534*, the T_{ave} values are 659 °C (606–699 °C) for Rt_{mtx}, 640 °C (565–683 °C) for Rt_{inc}, and 651 °C for a single R_{ovg} grain. Similar temperature values were obtained from the three textural varieties of rutile in *sample Ph537* (Table 1; Fig. 8). In a similar manner to other retrogressed eclogites, garnetites exhibit lower temperature values when compared with those exhibited by their fresh counterparts, and few grains show large deviation from T_{ave} (as much as ±75 °C) even though majority of the grains still ensures values of within ±25 °C (Fig. 9).

5.6. Garnet-amphibolites

In garnet amphibolites *sample Ph482*, 40 spots on three types of rutiles were analyzed. The textural features are denoted in Fig. 6e and f. The Zr contents are 253–425 ppm (average: 334 ppm, *n*: 12) in Rt_{mtx}, 140–483 ppm (average: 302 ppm, *n*: 15) in Rt_{inc}, and 64–387 ppm (average: 262 ppm, *n*: 13) in Rt_{ovg}. When compared with Rt_{mtx} and Rt_{inc}, Rt_{ovg} yielded lower Zr contents. Rt_{mtx} shows a narrow range (250–420 ppm) (Fig. 7). However, Rt_{inc} and Rt_{ovg} yielded a comparatively wider range of 100–480 ppm.

The T_{ave} values from *sample Ph482* were 665 °C (647–689 °C) for Rt_{mtx}, 661 °C (604–700 °C) for Rt_{inc}, and 640 °C (552–681 °C) for Rt_{ovg} (Table 1; Fig. 8). The results are similar to those observed in garnetites and highly retrogressed eclogites, and most of the data cluster within ±25 °C of T_{ave} with few grains that yielded values of lower than T_{ave} having ranges as high as ±100 °C (Fig. 9).

6. Discussion

6.1. Zr variation in the rutile textural types

The Zr contents in Rt_{mtx} were relatively homogeneous in majority of the investigated samples, however, a gradual decrease in Zr contents was observed in the retrogressed rocks (Fig. 7). The highly retrogressed eclogites (*sample Ph243*) showed large scatter in Rt_{mtx}. The Zr contents in Rt_{inc} dominantly overlap Rt_{mtx} in most samples except garnetites and garnet-amphibolites, where they show a wide range (Fig. 7). When compared with matrix and inclusion type rutile, Rt_{ovg} shows considerable heterogeneity. In UHP eclogites, we could analyze only two Rt_{ovg} grains, which exhibited similar compositions, therefore, the Zr variation could not be determined. All the three textural varieties of rutile in garnetites denote the lowest Zr contents among the analyzed samples. Although these garnetites are located near the UHP eclogites but they may have been undergone a high degree of retrogression. We also checked the variation of Zr within single rutile grains (where two or more spots were analyzed), but no significant change was observed, irrespective of their occurrence in the metamorphic suite, suggesting homogeneous chemical compositions at the individual grain scale (Fig. 10).

Zack et al. (2004) reported rutile inclusions in garnet with high Zr contents in eclogites from a variety of HP metamorphic terranes, attributed to the protection owing to the shielding effect of garnet, which preserved the peak metamorphic temperatures. The Rt_{mtx} with low Zr contents was likely to be reset during cooling under temperatures of 635 °C (Zack et al., 2004). In contrast, areas with faster cooling rates (100 °C/Ma) have been; such as Alpe Arami, Italy (Olker et al., 2003), reported where the Zr-in-rutile was not reset under T conditions of up to 800 °C. Zhang et al. (2009) reported low but homogeneous Zr contents in Rt_{inc} (in garnet and omphacite) and high Zr contents with large chemical variation in Rt_{mtx} from the CCSD eclogites. The Rt_{inc} represent peak or near-peak metamorphism, whereas matrix rutile was affected by fluid-infiltration during retrogression. Later studies (e.g., Kooijman et al., 2012; Pape et al., 2016) argued the shielding effect on the rutile inclusions and interpreted their Zr-in-rutile thermometry for peak metamorphism. Our data show similar chemical compositions of the Rt_{mtx} and Rt_{inc}, whereas Rt_{ovg} exhibit some scatter. Rutile grains with low Zr contents suggest those grains were either recrystallized through dissolution–reprecipitation or suffered from minor diffusion after the peak metamorphism. Experimental and empirical studies (e.g., Hayden and Watson, 2007; Pape et al., 2016) suggest that the Zr expelled from rutile was incorporated in the overgrowing ilmenite and/or titanite during cooling. Other studies reported micro-scale zircon growth around rutile grain-boundaries that indicate thermal disturbance during the cooling processes rather than diffusional activities (e.g., Bingen et al., 2001; Harley, 2008; Jiao et al., 2011; Kooijman et al., 2012; Watson et al., 2006; Zack et al., 2004).

Ewing et al. (2013) observed flat Zr profiles across the rutile grains in high-temperature rocks (~970 °C) of the IVZ, where the absence of a systematic drop in Zr contents along the rutile edges suggest a negligible diffusion effect. Several rutile grains, with an irregular Zr variation, contained tiny zircon exsolution needles that possibly affected the analytical results. However, a systematic relation could not be observed among the rutile grains (irrespective of their size) that could provide evidence of diffusion. Some studies (Harley, 2016; Hayden and Watson, 2007) suggested possible resetting of the Zr-poor rutile due to the dissolution–reprecipitation processes; however, no textural features demonstrating rutile recrystallization were presented. The available chemical and textural evidence suggest that such a mechanism would result in a relatively homogeneous and Zr-rich Rt_{mtx} as well as relatively heterogeneous Rt_{ovg}. Ilmenite and titanite rimming Rt_{ovg} can be interpreted as the breakdown of rutile during retrogression. The rutile inclusions containing low Zr contents may have been formed during

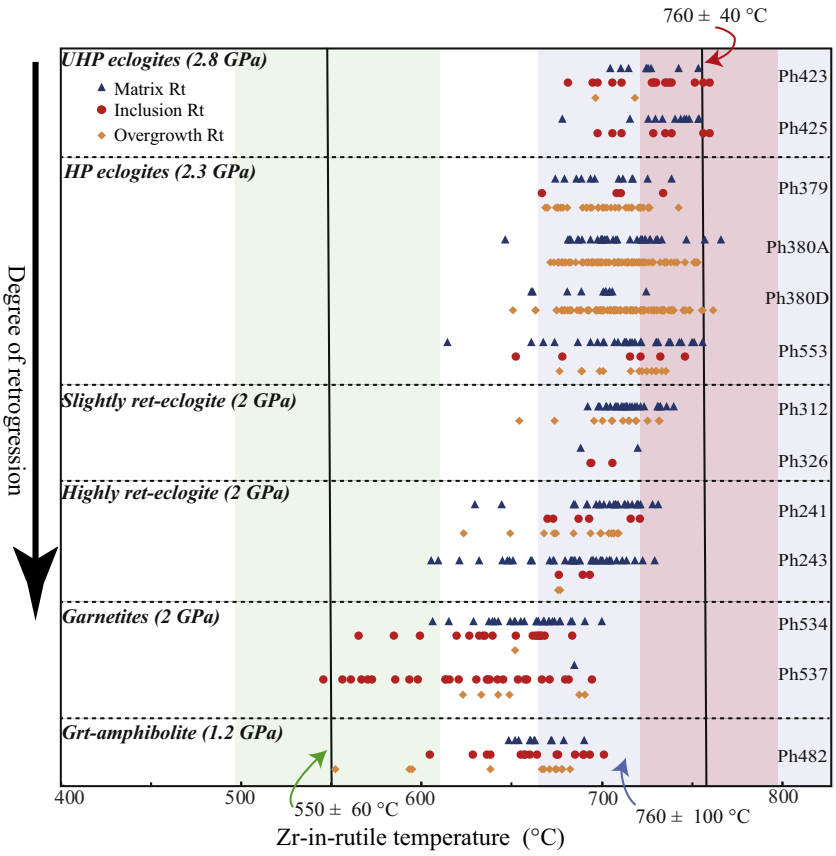

Fig. 8. A diagram displaying the Zr-in-rutile thermometry results for the analyzed samples. Note the homogeneous and the highest T values from the UHP eclogites among the analyzed samples. Pressure values were adopted from the previously reported conventional thermobarometry data (Rehman et al., 2007, 2013b). The shaded areas for 760 ± 40 °C, 760 ± 100 °C, and 550 ± 60 °C, represent the average T values of the UHP eclogites, HP eclogites, and amphibolites, respectively, previously determined by conventional thermobarometry. Vertical axis shows the degree of retrogression (increasing downward). The dashed horizontal lines differentiate different rock suites.

prograde metamorphism and acquired their Zr budget from the breakdown of hornblende or ilmenite from the precursor rocks.

We verified the Zr/Nb ratios in three textural varieties of rutile but observed no clear relation with the different textural occurrences, except for those observed in garnetites. The Nb contents in rutile in garnetites were significantly higher (as much as several thousand ppm) when compared with that in eclogites and their retrogressed counterparts (supplementary Table S1). The data suggest that the garnetites either had a different protolith from that of the eclogites or experienced considerable retrogression (and possibly a high degree of fluid ingress), facilitating Zr loss that was uptaken by the neighbouring ilmenite and/or titanite, whereas Nb remained in rutile because of the lack of Nb sink. High Nb contents have also been reported from the granulites in the IVZ (Luvizotto and Zack, 2009), the KB, China (Jiao et al., 2011), and in the amphibolites of the Catalina Schist, southern California (Kohn et al., 2016) that reflected diffusional resetting during the late metamorphic stages.

Kooijman et al. (2012) interpreted the Zr-poor and Nb-rich rutile from the APG to have crystallized during the prograde biotite breakdown. In garnetites, rutile inclusions, whether in full garnets or in outer domains of atoll garnets, are formed under conditions of low Zr and high Nb contents. The Zr contents in Rt_{mtx} and Rt_{ovg} were also low and show no systematic variation inside the grains (Fig. 10). These features indicate that garnetites are most likely to be reequilibrated after the post-peak decompression stage. Generally, atoll shaped garnets are formed by the partial resorption of the garnet cores due to the temperature increase owing to fluid infiltration (Cheng et al., 2007; Faryad et al., 2010; Smellie, 1974). However, Rt_{mtx} and Rt_{ovg} as well as rutile inclusions in full garnets and some atoll shaped garnets show lower Zr contents and yield lower temperatures when compared with those obtained from the HP and UHP eclogites. A further detailed study on garnetites is required to completely understand their origin.

6.2. Zr-in-rutile thermometry

The temperature values obtained from the UHP and HP eclogites agree with the previously reported values from conventional thermobarometry, falling within the range but lower than the maximum temperature values (Rehman et al., 2007, 2008, 2013b). These data reinforce the results obtained from other studies that have shown that Zr-in-rutile thermometry is a useful tool for high P–T metamorphic rocks. However, the fluid–rock interaction during the retrogression stages, recorded by the common presence of symplectitic textures, may reset the Zr budget. A number of rutile grains, whether in UHP eclogites or their retrogressed counterparts, apparently preserved the Zr contents reflecting peak metamorphic temperatures comparable with those obtained from conventional thermobarometry. In contrast, the partially or completely reset rutile grains yielded low temperature values. Although the temperatures obtained from the analyzed rutile exhibited a narrow range (550–750 °C), no systematic variation was observed with respect to the textural varieties, even at the individual grain level. The heterogeneous and low-Zr nature of Rt_{ovg} indicated that the Zr budget was likely to be shared by the associated ilmenite and/or titanite that texturally armored it. The formation of ilmenite by the breakdown of garnet and rutile during decompression by *grossular garnet + almandine garnet + rutile = ilmenite + anorthite + quartz* or *almandine garnet + rutile = ilmenite + sillimanite/andalusite + quartz* (Bohlen et al., 1983; Bohlen and Liotta, 1986; Frost, 1991) was reported by Pape et al. (2016) based on their study on natural rocks. We suggest that ilmenite may have formed by the breakdown of garnet and rutile in

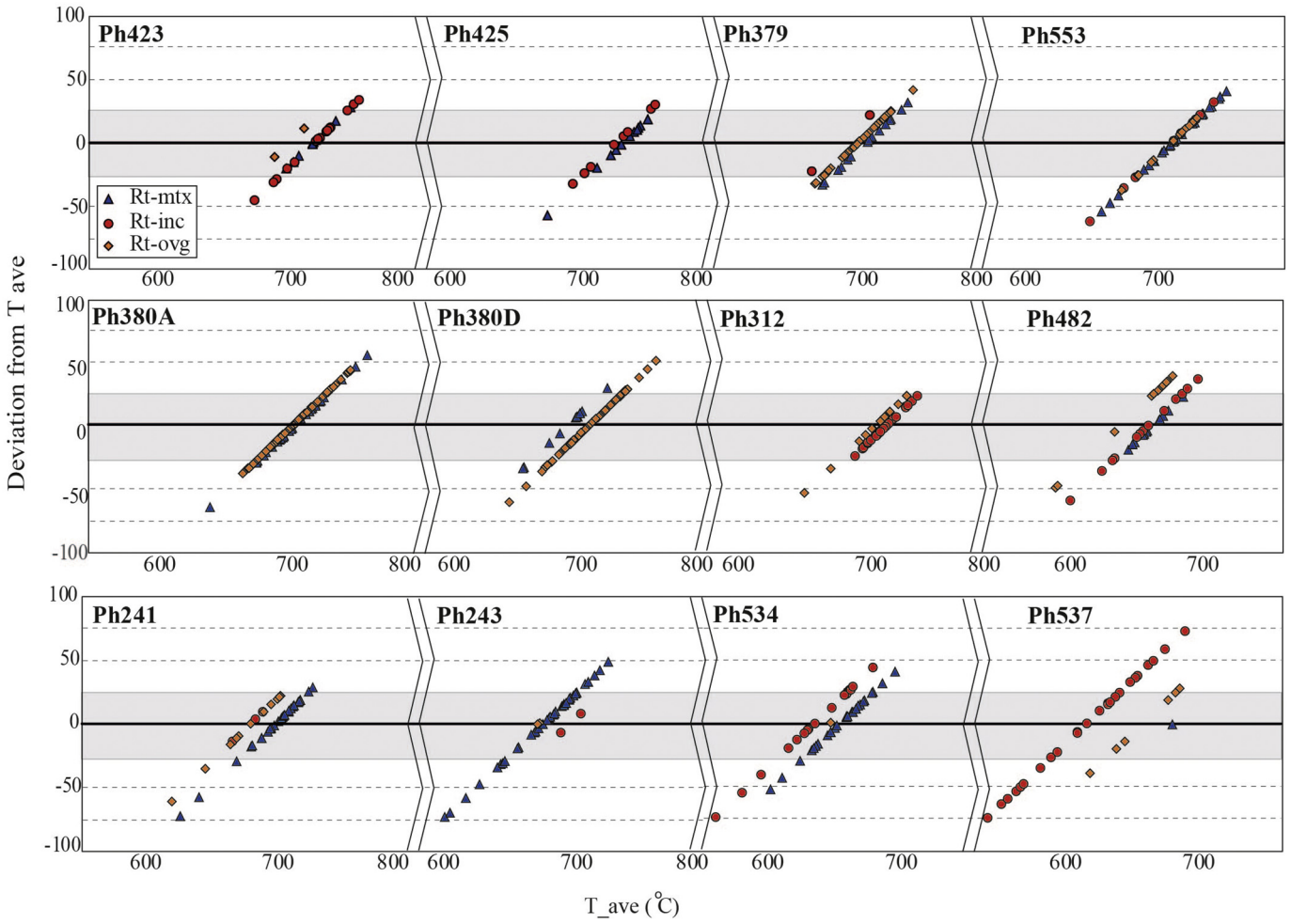

Fig. 9. Diagrams showing the T range along the horizontal axis for the analyzed rutile versus the temperature deviation from the average temperature along the vertical axis. The horizontal thick line in the middle of the plot represents zero difference from the average T. The deviation of the T values of the individual spots is ±25 °C (shaded area) from the average temperature for a particular sample; however, a few spots exceptionally show significant deviation.

the studied rocks via the first reaction during the post-peak cooling or decompression stages. In contrast, the experiments conducted on metagranites from the Italian Alps (Angiboust and Harlov, 2017) showed that rutile formed at the expense of ilmenite under high P–T conditions and titanite under low P–T conditions. Tual et al. (2018) also reported rutile grown at the expense of ilmenite during prograde metamorphism and noted that the same rocks contained ilmenite formed at the expense of Rt_{mtx} during the retrograde stage. The partial replacement of rutile by ilmenite and recrystallization of rutile likely reset the Zr contents and the metamorphic temperatures. Tual et al. (2018) did not find any evidence of Zr diffusion that could affect the temperature records. They denoted that the rutile in granulites can be affected by Zr loss because of the diffusion process when the crystallization temperatures exceeded the Zr diffusion closure temperature. Their data showed that Rt_{mtx} retained lower Zr contents and were likely produced by the breakdown of titanium-bearing hornblende during the dehydration stage.

Our study suggests that the Zr budget was acquired by Rt_{mtx} and Rt_{inc} from the breakdown of hornblende and ilmenite in the protoliths during the Indian Plate subduction-related prograde metamorphism. The high temperature data and homogenous chemical composition of Rt_{mtx} and Rt_{inc} in the UHP and HP eclogites reflect peak or near-peak metamorphic stages, whereas the low temperature data and heterogeneous chemical composition of Rt_{ovg} suggest reequilibration or partial resetting of the early-formed rutile during retrogression. These features are consistent with the textural features, where most of the peak metamorphic phases are retrogressed to form stable phases at low temperatures. In contrast, the Rt_{mtx} and Rt_{inc} in garnet and omphacite apparently retained the Zr contents from peak or near-peak conditions. Further, the Rt_{mtx} and Rt_{inc} in slightly retrogressed eclogites exhibited similar temperature values to those exhibited by their fresh HP and UHP eclogite analogues. Previous study showed high temperature estimates (~820 °C) from HP eclogites that Rehman et al. (2008) have interpreted as the post-eclogite decompression stage; however, the Zr-in-rutile thermometry has produced fairly homogeneous results, suggesting that Zr-in-rutile thermometry is applicable even in HP and UHP rocks strongly overprinted by retrogression. The homogeneous concentrations of Zr in Rt_{mtx} and Rt_{inc} possibly reflect equilibration coeval with garnet growth under peak eclogite-facies conditions. This is consistent with the lack of core-to-rim garnet zoning in UHP eclogites (Rehman et al., 2008, 2013b, 2017) and indicates that the Zr contents in Rt_{mtx} and Rt_{inc} reflect the original crystallization composition. Further, the indistinguishable temperature values are geologically meaningful. In case of HP eclogites, some of the garnet grains preserved prograde cores but we could not find the Rt_{inc} in these cores; therefore, majority of the temperature values determined from Rt_{mtx} and Rt_{inc} in HP eclogites reflected the near-peak eclogite-facies metamorphism. In contrast, Rt_{ovg}, denoting some spread in terms of the Zr contents, reflect post-peak cooling.

6.3. Zr diffusion in rutile

The evidence for the diffusion of trace elements (particularly HFSE) in rutile has been previously presented based on experimental and

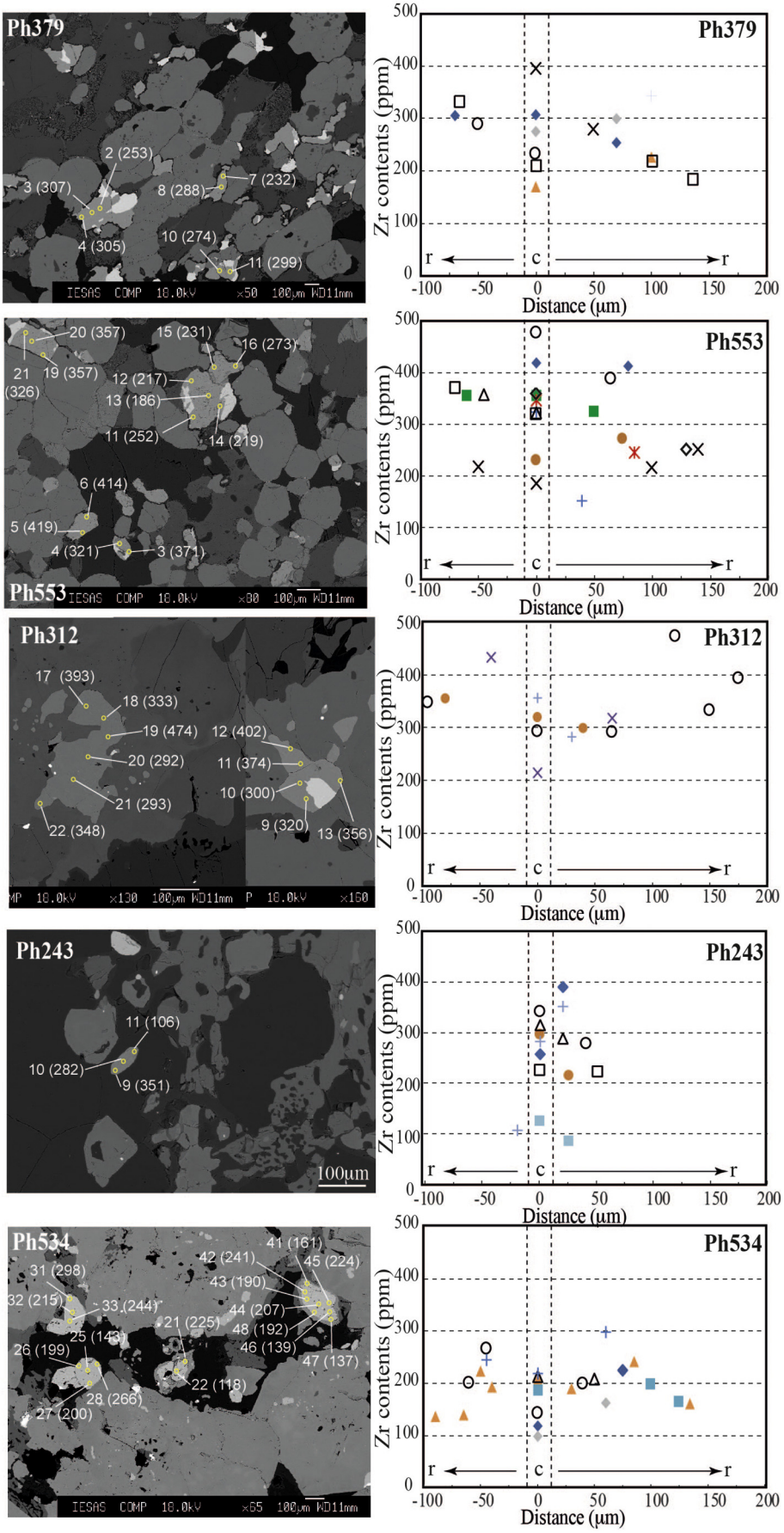

Fig. 10. Backscattered electron images of some of the analyzed rutiles (open circles mark the EPMA analysis performed). Numbers on the images represent the analysis spot# (as shown in the supplementary Table S1) and the digits in parenthesis show the Zr contents (ppm). The plots shown to the right display the Zr contents at the intra-grain scale. The cores of the grains are marked with the alphabet "c" and rims are shown as "r" on both sides of the grain (a distance with negative integers indicate the other side of the grain) from the center. No significant variation was observed in the Zr contents from the core to the rim.

empirical studies (e.g., Blackburn et al., 2012; Cherniak et al., 2007; Dohmen et al., 2018; Kohn and Penniston-Dorland, 2017; Lucassen et al., 2010; Marschall et al., 2013; Sasaki et al., 1985; Taylor-Jones and Powell, 2015; Zhu et al., 2017). Sasaki et al. (1985) conducted experiments (at 1100–1500 °C) on Zr diffusion in rutile as a function of temperature and oxygen partial pressure and observed that the diffusion rates of trace elements in rutile are five times larger in directions perpendicular to rather than along the c-axis. Their results denoted a positive correlation between the diffusion rate and temperature. Cherniak et al.'s (2007) experiments (at 750–1100 °C) on synthetic and natural rutile denoted slower rates of Zr diffusion in rutile when compared with those reported by Sasaki et al. (1985). In comparison with the diffusion of Ti-in-zircon, the rates were five times faster at ~770 °C and decreased during retrogression, maintaining equilibrium with the matrix quartz and zircon. They associated these temperatures with the peak metamorphic conditions. However, they warned that the Zr-in-rutile thermometry is less resistant to resetting than Zr-in-titanite or Ti-in-zircon and that it may also incorporate inter-grain Zr variability either from in-diffusion (incorporation of Zr from the matrix zircon along the rutile rim) or out-diffusion (Zr loss from the rutile due to dissolution–reprecipitation). Lucassen et al. (2010) observed core-to-rim diffusion-controlled enrichments of HFSE in rutile, denoting that the Zr contents were gradually affected by the diffusion along the rims surrounding the chemically uniform cores. However, no systematic variation could be observed along the grain boundaries, indicating effective diffusion (e.g., rutile–titanite). In another experimental study on Zr diffusion, Blackburn et al. (2012) observed that under fast-cooling conditions, rutile with uniform Zr contents initially retained high temperatures, while under slow-cooling conditions, as reflected in the decrease of Zr contents from the core to the rim, the diffusive loss of Zr was dominant. Taylor-Jones and Powell (2015) advised that the Zr diffusion in rutile may obliterate the metamorphic temperature records because the single-mineral thermometry is vulnerable to diffusional reequilibration upon cooling, and the peak metamorphic temperatures may not be preserved. As Zr-in-rutile thermometry works on the principle of equilibrium of the coexisting rutile + quartz + zircon, the occurrence of zircon close to rutile facilitates the loss of Zr from the rutile that could be taken in by zircon, resulting in erroneous temperatures. They concluded that if Zr was the rate-controlling species in rutile, the high temperatures obtained from the Zr-in-rutile thermometry would represent the peak metamorphic conditions. Similar interpretations were made by Kohn and Penniston-Dorland (2017) regarding diffusion in rutile and its effects on the Zr-in-rutile thermometry. Zhu et al. (2017) reported diffusion-related anisotropy in large atoms (including Zr and scandium (Sc)). They observed interstitial diffusion in which elements were exchanged via interstitial vacancies or open channels in the atomic structure along the c-axis and diffused via a kick-out mechanism (collision and replacement of elements) perpendicular to the c-axis. Dohmen et al. (2018) found indistinguishable diffusion profiles along the a-axis but some anisotropy along the c-axis that favored diffusion activation (at 800–1100 °C). Mitchell and Harley (2017) reported Zr-in-rutile temperatures of 606–780 °C at 1.1 GPa from the UHT granulites of the Napier Complex. Most of the analyzed rutile grains in their study exhibited flat core–rim Zr contents but some grains had zircon precipitates or exsolution rods along the grain boundaries, which they interpreted to be the evidence of recrystallization. By reintegrating the Zr contents in the recrystallized domains, they obtained temperatures of ~1149 °C, consistent with the peak metamorphic temperature estimated using other thermometers (~1100 °C). The low temperatures were interpreted to have been reset because of the fluid-mediated mobility of Zr in rutile during retrogression.

The aforementioned studies document the Zr diffusion in rutile, and majority of them advocate a concept that systematic chemical variation at the inter-grain or intra-grain level explains Zr diffusion; further, the temperatures determined from such grains will be affected. In contrast, the analyzed grains that are chemically homogeneous and have high Zr contents can be assumed to represent pristine and unaltered grains and, hence, potentially yield meaningful temperatures. We did not find a systematic variation in Zr (or in Nb) from the core to the margin in grains on the three textural varieties of rutile. Most of the analyzed grains exhibit an almost flat Zr pattern at the within-grain level (with minor grain-to-grain variation), indicating that the diffusion is insignificant. Majority of the Rt_{mtx} and Rt_{inc} grains preserved relatively high Zr contents and yielded temperature values consistent with the previously reported conventional thermobarometry values (Rehman et al., 2007, 2013a). We interpret those grains as indicative of the peak- or near-peak eclogite-facies conditions. In contrast, rutile grains with relatively low Zr contents are likely to be affected by chemical resetting during retrograde metamorphism, because of which the temperature values obtained from these grains are low. These grains also show no significant within-grain chemical variation and, hence, show no effect of diffusion loss but possibly lose their Zr using the kick-out mechanism proposed by Zhu et al. (2017) or by dissolution–reprecipitation similar to that proposed by previous authors (e.g., Harley, 2016; Hayden and Watson, 2007; Pape et al., 2016).

6.4. Metamorphic evolution

The metamorphic evolution from near-peak to peak (coesite stability field) conditions related to the subduction–collision of the Indian Plate and post-collisional exhumation-related retrogression can be constrained by the Zr-in-rutile thermometry combined with petrography and geochronology. The U-Pb zircon ages from the Kaghan Valley eclogites show peak UHP metamorphism at ~46 Ma (Kaneko et al., 2003; Rehman et al., 2013a, 2013b, 2016). Similar age data, ~44 Ma, were obtained from the rutile from the Kaghan Valley eclogites (Spencer and Gebauer, 1996) and were interpreted as the timing of the peak eclogite-facies metamorphism. Wilke et al. (2010) reported ages of 47–34 Ma (U-Pb zircon, Ar-Ar hornblende, and white mica), interpreted for peak metamorphism through post-peak rapid exhumation. Also, U-Pb zircon ages of 46 Ma from the coesite-bearing domain and 41 Ma from the quartz-bearing domain within the zircon from the host UHP felsic gneiss (Kaneko et al., 2003) indicate rapid exhumation from UHP (>95-km depth) to amphibolite-facies conditions (<60-km depth). The Rt_{mtx} and Rt_{inc} from the UHP/HP eclogites preserve peak- or near-peak metamorphic temperatures (~750 °C), whereas the lower temperatures (550–600 °C) of Rt_{ovg} and some Rt_{mtx} show post-peak resetting. Homogeneous grains with high Zr contents are chemically undisturbed, whereas grains with heterogeneous chemical compositions and low Zr contents suggest diffusive loss or have been recrystallized and reprecipitated during retrogression. In particular, the Rt_{ovg} rimmed by ilmenite and/or titanite are most likely to be reset. Rehman et al. (2014, 2018) supported chemical resetting in the highly retrogressed eclogites based on the oxygen-isotope data. The UHP eclogites preserved negative $\delta^{18}O$ values from their protoliths, unaffected by retrogression, whereas positive $\delta^{18}O$ values in retrogressed rocks indicate progressive fluid–rock interaction. The Zr-in-rutile thermometry data for the Himalayan eclogites are consistent with other textural and geochemical results, reflecting a polymetamorphic history.

7. Conclusions

The relatively indistinguishable chemical compositions and comparable temperature values of Rt_{mtx} and Rt_{inc} can be attributed to the near-peak UHP/HP metamorphism, and retrograde metamorphism did not mobilize the Zr in rutile. However, the Rt_{ovg} and some of the Rt_{mtx} may have recrystallized by dissolution–reprecipitation during retrogression. The Zr expelled by the breakdown of the earlier-formed rutile was shared by the overgrowing phases, including ilmenite or titanite, consistent with the textural relation of ilmenite or titanite armoring the Rt_{ovg}. Our data suggest that Zr-in-rutile thermometry is useful to extract the peak or near-peak metamorphic temperatures from rocks

having polymetamorphic history. However, the late-stage cooling events are likely to affect the metamorphic records, particularly grains that have been modified by diffusion or dissolution–reprecipitation. Careful inspection of the textures and compositional variations is required for distinguishing between pristine and chemically disturbed rutile before interpreting the metamorphic records.

Supplementary data to this article can be found online at https://doi.org/10.1016/j.lithos.2019.06.017.

Acknowledgements

We thank Emily Hung, Terry Tan, and Chung Xiao for their help in the sample preparation and analysis. We appreciate critical comments by two anonymous reviewers which improved the manuscript significantly. We thank John Wakabayashi and Bo Causer for their help in improving the language. This work was supported by the Taiwan MOST fund (Project# 1050021585 to S-LC) and the JSPS research fund (Kakenhi # 15K05316 to HUR).

References

Angiboust, S., Harlov, D., 2017. Ilmenite breakdown and rutile-titanite stability om metagranitoids: Natural observations and experimental results. Am. Mineral. 102, 1696–1708.
Bingen, B., Austrheim, H., Whitehouse, M., 2001. Ilmenite as a source for zirconium during high-grade metamorphism? Textural evidence from the Caledonides of western Norway and implications for zircon geochronology. J. Petrol. 42, 355–375.
Blackburn, T., Shimizu, N., Bowring, S.A., Schoene, B., Mahan, K.H., 2012. Zirconium in rutile speedometry: new constraints on lower crustal cooling rates and residence temperatures. Earth Planet. Sci. Lett. 317-318, 231–240.
Bohlen, S.R., Liotta, J.J., 1986. A barometer for garnet amphibolites and garnet granulites. J. Petrol. 27, 1025–1034.
Bohlen, S.R., Wall, V.J., Boettcher, A.L., 1983. Experimental investigations and geological applications of equilibria in the system FeO-TiO_2-Al_2O_3-SiO_2-H_2O. Am. Mineral. 68, 1049–1058.
Chaudhry, M.N., Ghazanfar, M., 1987. Geology, structure and geomorphology of upper Kaghan Valley, North western Himalaya, Pakistan. Geol. Bull. Univ. Punjab 22, 13–57.
Cheng, H., Nakamura, E., Kobayashi, K., Zhou, Z., 2007. Origin of atoll garnets in eclogites and implications for the redistribution of trace elements during slab exhumation in a continental subduction zone. Am. Mineral. 92, 1119–1129.
Cherniak, D.J., Manchester, J., Watson, E.B., 2007. Zr and Hf diffusion in rutile. Earth Planet. Sci. Lett. 261, 267–279.
Connolly, J.A.D., 1990. Multivariable phase-diagrams - an algorithm based on generalized thermodynamics. Am. J. Sci. 290, 666–718.
Connolly, J.A.D., 2005. Computation of phase equilibria by linear programming: a tool for geodynamic modelling and its application to subduction zone decarbonation. Earth Planet. Sci. Lett. 236, 524–541.
Connolly, J.A.D., 2009. The geodynamic equation of state: what and how. Geochem. Geophys. Geosyst. 10, Q10014. https://doi.org/10.1029/2009GC002540.
Cruz-Uribe, A.M., Feineman, M.D., Zack, T., Jacob, D.E., 2018. Assessing trace element (dis) equilibrium and the application of single element thermometers in metamorphic rocks. Lithos 314-315, 1–15.
de Capitani, C., Brown, T.H., 1987. The computation of chemical equilibrium in complex systems containing non-ideal solutions. Geochim. Cosmochim. Acta 51, 2639–2652.
de Capitani, C., Petrakakis, K., 2010. The computation of equilibrium assemblage diagrams with Theriak/Domino software. Am. Mineral. 95, 1006–1016.
Degeling, H., Ellis, D., Williams, I.S., 2002. Textural and isotopic constraint on zircon formation during cooling of the Napier Complex, East Antarctica. 18th IMA. Programme with Abstracts, p. 235.
Dohmen, R., Marschall, H.R., Ludwig, T., Polednia, J., 2018. Diffusion of Zr, Hf, Nb and Ta in rutile: effects of temperature, oxygen fugacity, and doping level, and relation to rutile point defect chemistry. Phys. Chem. Miner. https://doi.org/10.1007/s00269-018-1005-7.
Ewing, T.A., Hermann, J., Rubatto, D., 2013. The robustness of the Zr-in-rutile and Ti-in-zircon thermometers during high-temperature metamorphism (Ivrea-Verbano Zone, northern Italy). Contrib. Mineral. Petrol. 165, 757–779.
Faryad, S.W., Klápová, H., Nosál, L., 2010. Mechanism of formation of atoll garnet during high-pressure metamorphism. Mineral. Mag. 74, 111–126.
Ferry, J.M., Watson, E.B., 2007. New thermodynamic models and revised calibrations for the Ti-in-zircon and Zr-in-rutile thermometers. Contrib. Mineral. Petrol. 154, 429–437.
Frost, B.R., 1991. Stability of oxide minerals in metamorphic rocks. In: Lindsley, D.H. (Ed.), Oxide Minerals: Petrological and Magnetic Significance. Reviews in Mineralogy 25, pp. 469–488.
Gansser, A., 1964. Geology of the Himalayas. Interscience Publishers, London, p. 289.
Greco, A., Spencer, D.A., 1993. A section through the India Plate, Kaghan Valley, NW Himalaya, Pakistan. In: Treloar, P.J., Searle, M.P. (Eds.), Himalayan Tectonics Geological Society of London. vol. 74, pp. 221–236 London, Special Publication.
Greco, A., Martinotti, G., Papritz, K., Ramsay, J.G., Rey, R., 1989. The Himalayan crystalline rocks of the Kaghan Valley (NE-Pakistan). Eclogae Geol. Helv. 82 (2), 603–627.
Green, T.H., Helman, P.L., 1982. Fe–Mg partitioning between coexisting garnet and phengite at high pressure, and comments on a garnet– phengite geothermometer. Lithos 15, 253–266.
Hacker, B., 2006. Pressures and temperatures of ultrahigh-pressure metamorphism: implications for UHP tectonics and H_2O in subducting slabs. Int. Geol. Rev. 48, 1053–1056.
Harley, S.L., 2008. Refining the P–T records of UHT crustal metamorphism. J. Metamorph. Geol. 26, 125–154.
Harley, S.L., 2016. A matter of time: the importance of the duration of UHT metamorphism. J. Mineral. Petrol. Sci. 111, 50–72.
Hayden, L.A., Watson, E.B., 2007. Rutile saturation in hydrous siliceous melts and its bearing on Ti-thermometry of quartz and zircon. Earth Planet. Sci. Lett. 258, 561–568.
Holland, T.J.B., Powell, R., 1998. An internally-consistent thermodynamic dataset for phases of petrological interest. J. Metamorph. Geol. 16, 309–344.
Holland, T.J.B., Powell, R., 2006. Petrological calculations involving Fe-Mg equipartition in multisite minerals: a logical inconsistency. J. Metamorph. Geol. 24, 851–861.
Jiao, S., Guo, J., Mao, Q., Zhao, R., 2011. Application of Zr-in-rutile thermometry: a case study from ultrahigh-temperature granulites of the Khondalite belt, North China Craton. Contrib. Mineral. Petrol. 162, 379–393.
Kaneko, Y., Katayama, I., Yamamoto, H., Misawa, K., Ishikawa, M., Rehman, H.U., Kausar, A.B., Shiraishi, K., 2003. Timing of Himalayan ultrahigh-pressure metamorphism: sinking rate and subduction angle of the Indian continental crust beneath Asia. J. Metamorph. Geol. 21, 589–599.
Kohn, M.J., 2014. Himalayan metamorphism and its tectonic implications. Annu. Rev. Earth Planet. Sci. 42, 381–419.
Kohn, M.J., Penniston-Dorland, S.C., 2017. Diffusion: obstacles and opportunities in petrochronology. Rev. Mineral. Geochem. 83, 103–152.
Kohn, M.J., Penniston-Dorland, S.C., Ferreira, J.C.S., 2016. Implications of near-rim compositional zoning in rutile for geothermometry, geospeedometry, and trace element equilibration. Contrib. Mineral. Petrol. 171, 78. https://doi.org/10.1007/s00410-016-1285-1.
Kooijman, E., Smit, M.A., Mezger, K., Berndt, J., 2012. Trace element systematics in granulite facies rutile: implications for Zr geothermometry and provenance studies. J. Metamorph. Geol. 30, 397–412.
Krogh Ravna, E.J., 1988. The garnet–clinopyroxene Fe–Mg geothermometer: a reinvestigation of existing experimental data. Contrib. Mineral. Petrol. 99, 44–48.
Krogh Ravna, E.J., Raheim, A., 1978. Temperature and pressure dependence of Fe–Mg partitioning between garnet and phengite, with particular reference to eclogites. Contrib. Mineral. Petrol. 66, 75–80.
Krogh Ravna, E.J., Terry, M.P., 2004. Geothermobarometry of UHP and HP eclogites and schists – an evaluation of equilibria among gannet-clinopyroxene-kyanite-phengite-coesite /quartz. J. Metamorph. Geol. 22, 579–592.
Lombardo, B., Rolfo, F., 2000. Two contrasting eclogite types in the Himalaya: implications for the Himalayan orogeny. J. Geodyn. 30, 37–60.
Lucassen, F., Dulski, P., Abart, R., Franz, G., Rhede, D., Romer, R.L., 2010. Redistribution of HFSE elements during rutile replacement by titanite. Contrib. Mineral. Petrol. 160, 279–295.
Luvizotto, G.L., Zack, T., 2009. Nb and Zr behaviour in rutile during high-grade metamorphism and retrogression: an example from Ivrea-Verbano Zone. Chem. Geol. 261, 303–317.
Luvizotto, G.L., Zack, T., Meyer, H.P., Ludwig, T., Triebold, S., Kronz, A., Munker, C., Stockli, S., Prowatke, S., Klemme, S., Jacob, D.E., von Eynatten, H., 2009. Rutile crystals as potential trace element and isotope mineral standards for microanalysis. Chem. Geol. 261, 346–369.
Marschall, H.R., Dohmen, R., Ludwig, T., 2013. Diffusion-induced fractionation of niobium and tantalum during continental crust formation. Earth Planet. Sci. Lett. 375, 361–371.
Miller, C., Zanetti, A., Thöni, M., Konzett, J., 2007. Eclogitization of gabbroic rocks: Redistribution of trace elements and Zr in rutile thermometry in an Eo-Alpine subduction zone (Eastern Alps). Chem. Geol. 239, 96–123.
Mitchell, R.J., Harley, S.M., 2017. Zr-in-rutile resetting in aluminosilicate bearing ultrahigh temperature granulites: refining the record of cooling and hydration in the Napier Complex, Antarctica. Lithos 272-273, 128–146.
O'Brien, P.J., Zotov, N., Law, R., Khan, M.A., Jan, M.Q., 2001. Coesite in Himalayan eclogite and implications for models of India–Asia collision. Geology 29, 435–438.
Olker, B., Altherr, R., Paquin, J., 2003. Fast exhumation of the ultrahigh-pressure Alpe Arami garnet peridotite (Central Alps, Switzerland): constraints from geospeedometry and thermal modelling. J. Metamorph. Geol. 21, 395–402.
Pape, J., Mezger, K., Robyr, M., 2016. A systematic evaluation of the Zr-in-rutile thermometer in ultra-high temperature (UHT) rocks. Contrib. Mineral. Petrol. 171, 44. https://doi.org/10.1007/s00410-016-1254-8.
Pognante, U., Spencer, D.A., 1991. First record of eclogites from the High Himalayan belt, Kaghan Valley (northern Pakistan). Eur. J. Mineral. 3, 613–618.
Powell, R., Holland, T.J.B., 2008. On thermobarometry. J. Metamorph. Geol. 26, 155–179.
Powell, R., Holland, T.J.B., Worley, B., 1998. Calculating phase diagrams involving solid solutions via non-linear equations, with examples using THERMOCALC. J. Metamorph. Geol. 16, 577–588.
Reed, S.J.B., 1993. Electron Microprobe Analysis. 2nd ed. Cambridge University Press, Cambridge 326 pp.
Rehman, H.U., 2019. Geochronological enigma of the HP–UHP rocks in the Himalayan orogen. In: Zhang, L.F., Schertl, H.-P., Wei, C.J. (Eds.), HP–UHP Metamorphism and Tectonic Evolution of Orogenic Belts. Geological Society of London, Special Publication vol. 474, pp. 183–207.
Rehman, H.U., Yamamoto, H., Kaneko, Y., Kausar, A.B., Murata, M., Ozawa, H., 2007. Thermobaric structure of the Himalayan metamorphic belt in Kaghan Valley, Pakistan. J. Asian Earth Sci. 29, 390–406.

Rehman, H.U., Yamamoto, H., Nakamura, E., Khalil, M.A., Zafar, M., Khan, T., 2008. Metamorphic history and tectonic evolution of the Himalayan UHP eclogites in Kaghan Valley, Pakistan. J. Mineral. Petrol. Sci. 103, 242–254.

Rehman, H.U., Seno, T., Yamamoto, H., Khan, T., 2011. Timing of collision of Kohistan–Ladakh arc with India and Asia: debate. Island Arc 20, 308–328.

Rehman, H.U., Kobayashi, K., Tsujimori, T., Ota, T., Yamamoto, H., Nakamura, E., Kaneko, Y., Khan, T., Terabayashi, M., Yoshida, K., Hirajima, T., 2013a. Ion microprobe U–Th–Pb geochronology and study of micro-inclusions in zircon from the Himalayan high and ultrahigh-pressure eclogites, Kaghan Valley of Pakistan. J. Asian Earth Sci. 63, 179–196.

Rehman, H.U., Yamamoto, H., Shin, K., 2013b. Metamorphic P–T evolution of high pressure eclogites from garnet growth and reaction textures: insights from the Kaghan Valley transect, northern Pakistan. Island Arc 22, 4–24.

Rehman, H.U., Tanaka, R., O'Brien, P.J., Kobayashi, K., Tsujimori, T., Nakamura, E., Yamamoto, H., Khan, T., Kaneko, Y., 2014. Oxygen isotopes in Indian Plate eclogites (Kaghan Valley, Pakistan): negative δ18O values from a high latitude protolith reset by Himalayan metamorphism. Lithos 208–209, 471–483.

Rehman, H.U., Lee, H.Y., Chung, S.L., Khan, T., O'Brien, P.J., Yamamoto, H., 2016. Source and mode of the Permian Panjal Trap magmatism: evidence from zircon U-Pb and Hf isotopes and trace element data from the Himalayan ultrahigh-pressure rocks. Lithos 260, 286–299.

Rehman, H.U., Jan, M.Q., Khan, T., Yamamoto, H., Kaneko, Y., 2017. Varieties of the Himalayan eclogites: a pictorial review of textural and petrological features. Island Arc 26 (e12209), 1–14. https://doi.org/10.1111/iar.12209.

Rehman, H.U., Kitajima, K., Valley, J.W., Lee, H.Y., Chung, S.L., Yamamoto, H., Khan, T., 2018. Low-$\delta^{18}O$ mantle-derived magma in Panjal traps overprinted by hydrothermal alteration and Himalayan UHP metamorphism: revealed by SIMS zircon analysis. Gondwana Res. 56, 12–22.

Sasaki, J., Peterson, N.L., Hoshino, K., 1985. Tracer impurity diffusion in single-crystal rutile (TiO2-x). J. Phys. Chem. Solids 46, 1267–1283.

Searle, M.P., Khan, M.A., Fraser, J.E., Gough, S.J., Jan, M.Q., 1999. The Tectonic Evolution of the Kohistan-Karakoram Collision Belt along the Karakoram Highway Transect, North Pakistan Tectonics. vol. 18 pp. 929–949.

Smellie, J.A.T., 1974. Formation of atoll garnets from the aureole of the Ardara pluton, Co. Donegal, Ireland. Mineral. Mag. 39, 878–888.

Spear, F.S., 1993. Metamorphic Phase Equilibria and Pressure–Temperature–Time Paths. Mineralogical Society of America, Washington, D. C, p. 799.

Spencer, D.A., Gebauer, D., 1996. SHRIMP evidence for a Permian protolith age and a 44 Ma metamorphic age for the Himalayan eclogites (Upper Kaghan, Pakistan): implication for the subduction of the Tethys and the subdivision terminology of the NW Himalaya: Himalayan–Karakoram–Tibet Workshop, 11th, (Flagstaff, Arizona, USA). Abstract volume. pp. 147–150.

Stípská, P., Powell, R., 2005. Constraining the P–T path of a MORB-type eclogite using pseudosections, garnet zoning and garnet-clinopyroxene thermometry: an example from the Bohemian Massif. J. Metamorph. Geol. 23, 725–743.

Tahirkheli, R.A.K., 1979. Geology of Kohistan and adjoining area Eurasian and Indo-Pakistan continents, Pakistan. Geol. Bull. Univ. Peshawar (Special Issue) 15, 1–51.

Taylor, R.J.M., Kirkland, C.L., Clark, C., 2016. Accessories after the facts: Constraining the timing, duration and conditions of high-temperature metamorphic processes. Lithos 264, 239–257.

Taylor-Jones, K., Powell, R., 2015. Interpreting zirconium-in-rutile thermometric results. J. Metamorph. Geol. 33, 115–122.

Tomkins, H.S., Powell, R., Ellis, D.J., 2007. The pressure dependence of the zirconium-in-rutile thermometer. J. Metamorph. Geol. 25, 703–713.

Treloar, P.J., 1995. Pressure–temperature–time paths and the relationship between collision, deformation and metamorphism in the north-west Himalaya. Geol. J. 30, 333–348.

Treloar, P.J., 1997. Thermal controls on early-Tertiary, short-lived, rapid regional metamorphism in the NW Himalaya, Pakistan. Tectonophysics 273, 77–104.

Treloar, P.J., O'Brien, P.J., Parrish, R.R., Khan, M.A., 2003. Exhumation of Early Tertiary, coesite-bearing eclogites from the Pakistan Himalaya. J. Geol. Soc. Lond. 160, 367–376.

Tual, L., Möller, C., Whitehouse, M.J., 2018. Tracking the prograde P–T path of Precambrian eclogite using Ti-in-quartz and Zr-in-rutile geothermobarometry. Contrib. Mineral. Petrol. 173, 56. https://doi.org/10.1007/s00410-018-1482-1.

Usuki, T., Iizuka, Y., Hirajima, T., Svojtka, M., Lee, H.-Y., Jahn, B.-M., 2017. Significance of Zr-in-Rutile thermometry for deducing the decompression P–T path of a garnet-clinopyroxene granulite in the Maldanubian Zone of the Bohemian Massif. J. Petrol. 58, 1173–1198.

Watson, E.B., Wark, D.A., Thomas, J.B., 2006. Crystallization thermometers for zircon and rutile. Contrib. Mineral. Petrol. 151, 413–433.

Wei, C.J., Tian, Z.L., 2014. Modelling of the phase relations in high-pressure and ultrahigh-pressure eclogites. Island Arc 23, 254–262.

Wei, C.J., Powell, R., Zhang, L.F., 2003. Eclogites from the south Tianshan, NW China: Petrologic characteristic and calculated mineral equilibria in the Na2O–CaO–FeO–MgO–Al2O3–SiO2–H2O system. J. Metamorph. Geol. 21, 163–179.

Wilke, F.D.H., O'Brien, P.J., Gerdes, A., Timmerman, M.J., Sudo, M., Khan, M.A., 2010. The multistage exhumation history of the Kaghan Valley UHP series, NW Himalaya, Pakistan from U-Pb and 40Ar/39Ar ages. Eur. J. Mineral. 22, 703–719.

Zack, T., Kooijman, E., 2017. Petrology and geochronology of rutile. Rev. Mineral. Geochem. 83, 443–467.

Zack, T., Luvizotto, G.L., 2006. Application of rutile thermometry to eclogites. Mineral. Petrol. 88, 69–85.

Zack, T., Foley, S.F., Rivers, T., 2002. Equilibrium and disequilibrium trace element partitioning in hydrous eclogites (Trescolmen, Central Alps). J. Petrol. 43, 1947–1974.

Zack, T., Moraes, R., Kronz, A., 2004. Temperature dependence of Zr in rutile: empirical calibration of a rutile thermometer. Contrib. Mineral. Petrol. 148, 471–488.

Zhang, R.Y., Iizuka, Y., Ernst, W.G., Liou, J.G., Xu, Z.-Q., Tsujimori, T., Lo, C.-H., Jahn, B.-M., 2009. Metamorphic P–T conditions and thermal structure of Chinese continental scientific drilling main hole eclogites: Fe–Mg partitioning thermometer vs. Zr-in-rutile thermometer. J. Metamorph. Geol. 27, 757–772.

Zhu, L., Ackland, G., Hu, Q.-M., Zhou, J., Sun, Z., 2017. Origin of the abnormal diffusion of transition metal atoms in rutile. Phys. Rev. B 95, 245201.